

# Comparative Study on Fatigue Properties of Friction Stir Welding Joint and Lap Joint

**Teng Zhang<sup>1</sup>, Yuting He<sup>1,\*</sup>, Qing Shao<sup>1</sup>, Haiwei Zhang<sup>1</sup>, Liming Wu<sup>1</sup>**

<sup>1</sup> Aeronautics and Astronautics Engineering College, Air Force Engineering University, Xi'an 710038, China

\* Corresponding author: hyt666@tom.com

---

**Abstract** Friction Stir Welding (FSW) is a new type of solid-state connection which can reduce structural weight significantly. In this paper, fatigue tests and finite element analysis were employed to study fatigue properties of aerial aluminum alloy 2524-T3 FSW joint and lap joint. The S-N curves of specimens show that the fatigue strength of FSW joint is better than that of lap joint. Finite element models of two joints were established by ANSYS software. The residual stress of FSW joint were obtained by a nonlinear direct coupled-field analysis, and the detailed stress distribution of lap joint which under pulling force were simulated. On the basis of finite element analysis results, the fatigue lives of two types of joints were estimated. It is verified that the analytic and estimated results agree with that of experiment. The residual stress is the main factor affecting the fatigue life of FSW joint and the failure of lap joint is mainly caused by stress concentration of hole edge.

**Keywords** Friction stir welding, Fatigue test, S-N curve, Finite element analysis, Lap joint

---

## 1. Introduction

Friction stir welding (FSW) [1] is a new solid-state joining technology invented at the welding institute (TWI) of Britain in 1991. It is a technique well suit for joining many hard-to-weld metals without filler materials. Compared with traditional bolt or rivet jointing techniques, FSW can reduce connective weight significantly and has higher link efficiency. In order to reduce design, manufacture, and maintenance costs, FSW is applied to the fabrication of aircraft primary structures. In North America, Eclipse Aviation has developed the Eclipse 500 business jet, utilizing FSW in both wing and fuselage skin-stiffener-frame fabrication [2].

Extensive research has been carried out on FSW with the wide application of this technology. In order to improve the mechanical properties of FSW joint, many studies have been performed on welding procedure and microstructure of joint, and many researchers have explored the thermomechanical numerical simulation technology of FSW.

Thermal and mechanical behaviors are mutually dependent during the FSW process. Many researchers [3-7] have simulated this process by finite element method and have obtained the distribution of residual stress, but they didn't discuss the relationship between residual stress and fatigue life of FSW joint. Furthermore, reference [8] pointed out that the influence of residual stress on fatigue life of FSW joint is a problem need to be solved.

Reference [9] has studied the fatigue properties of aerial aluminum alloy 2524-T3 base metal specimens and three different sizes of FSW joints, fatigue tests have been carried out and the S-N curves have been obtained. Although the fatigue properties of base metal specimens and FSW joints have been compared, the fracture mechanism of FSW joints has not been identified.

Nowadays, structures such as skins and stringers are jointed together by bolts or rivets in most aircrafts, however, the comparative study on fatigue properties of FSW joint and bolt or rivet

connected joint is rare. In this paper, fatigue tests and finite element analysis (FEA) were employed to study the fatigue properties of 2524-T3 FSW joint and riveted lap joint. Test results show that the fatigue strength of FSW joint is better than that of lap joint. The residual stress of FSW joint and the detailed stress distribution of lap joint were obtained by FEA. Furthermore, the fatigue life of FSW joint was estimated according to the result of residual stress distribution and base metal S-N curve; the fatigue life of lap joint was estimated according to the results of stress-strain distribution and local stress-strain method.

## 2. Experiments

Fatigue tests of FSW joint specimens and lap joint specimens were made by machine MTS-810-500 at room temperature, just as shown in Fig.1 and Fig.2.



Figure 1. Fatigue test of FSW joint specimen    Figure 2. Fatigue test of lap joint specimen

### 2.1. Specimens and Fixture Design

Two types of specimens, which simulate different connective types of skins in airframe, are shown in Fig.3 and Fig.4. Pieces of specimens are made of aluminum alloy 2524-T3 and rivets are made of titanium alloy TC4. FSW joint specimens were produced by machine FSW2-4CX-006. The tool shoulder diameter is 8mm. The pin is cylindrical with a hemispherical tip, its dimensions are 2.6mm in diameter and in 1.7 mm length. The tool rotation speed is set at 1000 rpm, and the translation speed is fixed at 100mm/min. While the rotating tool moves along the welding line, a forging pressure of 1.5kN is applied. Lap joint specimens are connected by staggered rivets.

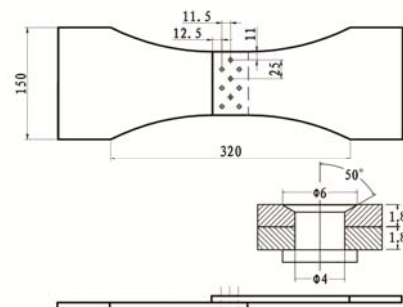
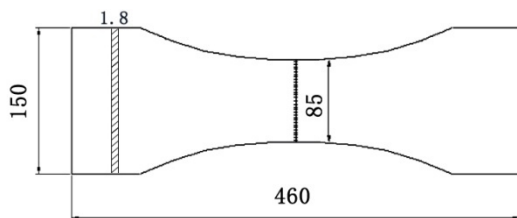


Figure 3. FSW joint specimen (mm)    Figure 4. Staggered riveted lap joint specimen (mm)

The weight of lap joint specimen and FSW joint specimen are 297g and 271g separately. This means the FSW technique could reduce structural weight significantly than traditional jointing techniques.

For the purpose of simulating the actual force condition, anti-bend fixtures were designed for lap joint specimens, just as shown in Fig.5. The anti-bend fixture I and II are designed to prevent out-of-plane bending and the function of shims is to ensure specimens loaded in the same plane. In order to reduce the friction between specimens and fixtures during test, some effective measures were applied such as injecting lubricant oil or inserting plastic films between contact surfaces.

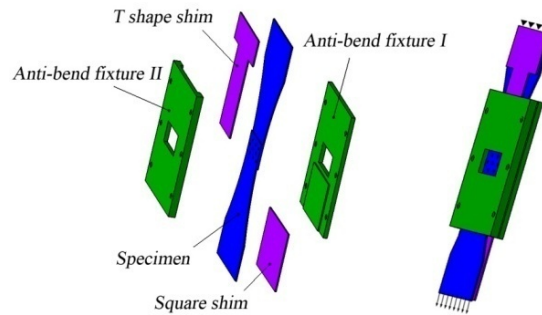


Figure 5. Configuration of anti-bend fixtures

## 2.2 Fatigue test

All specimens were subjected to constant amplitude loads; the stress ratio  $R=0.06$  and the load frequency  $f=10$ . In order to obtain S-N curves, each type of specimens were divided into three groups, which loaded under different stress levels (illustrated in Table 1).

Table 1. The maximum stress endured by different types of specimens during fatigue test (MPa)

	FSW specimen	Lap joint specimen
1	240	150
2	210	120
3	180	100

## 2.3 Test results

Fig.6 shows the fracture forms of specimens. The fracture position of FSW specimens locates on the thermomechanical affected zone and the lap joint specimens break on the line of the first row of rivets.

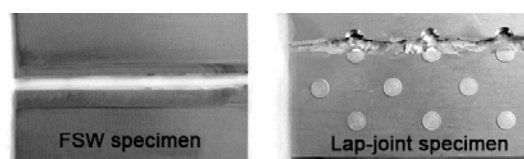


Figure 6. Fracture forms of two type specimens

*Chauvenet* criterion was used for all test results to abandon dubious data. And S-N curves of two

type specimens were obtained by group test method, the formulas of S-N curves are,

$$\text{FSW specimen: } N=1.89 \times 10^{11} (S-122)^{-3.36}, \quad (1)$$

$$\text{Lap joint specimen: } N=1.18 \times 10^8 (S-72.9)^{-1.84}. \quad (2)$$

S-N curves are illustrated in Fig.7.

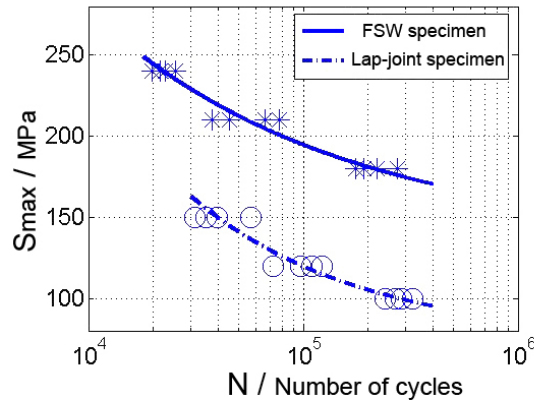


Figure 7. S-N curves of two type specimens

The S-N curves show that the fatigue strength of FSW joint is better than that of lap joint. At the fatigue life of  $1 \times 10^5$  cycles, the fatigue strength of FSW joint (195MPa) is about 61% higher than that of lap joint(120MPa).

### 3. Finite element analysis

In order to reveal the fracture mechanism of two jointing techniques, three-dimensional elasticplastic FEA for two types of specimens was conducted by ANSYS 14.0 software.

Through FEA, the residual stress of FSW joint and detailed stress distribution of lap joint were obtained, and both of them provide necessary conditions for life prediction.

#### 3.1 FEA of FSW joint

FSW is a coupled-field (structural-thermal) process. The temperature field affects the stress distribution during the entire process. Also, heat generated in structural deformation affects the temperature field. In this paper, a direct FEA of coupling is developed using a coupled-field element SOLID226. The simulation occurs over three load steps, representing the dwell, traverse and cool phases. The schematic diagram of FEA model is shown in Fig.8.

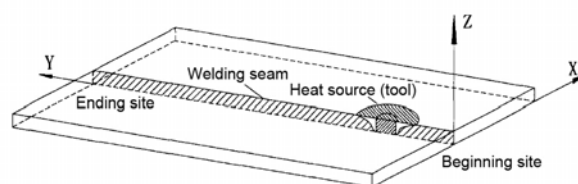


Figure 8. Schematic diagram of FEA model

The material properties of aluminum alloy 2524-T3 are shown in Table 2.

Table 2. Material properties of aluminum alloy 2524-T3

Temperature(°C)	25	150	300	500
Young's modulus(GPa)	68	60	51	38
Poisson's ratio	0.31	0.32	0.33	0.35
Density(kg/m <sup>3</sup> )	2810	2785	2750	2708
Coefficient of thermal expansion(um/m°C)	23	25.5	29	33
Yield stress(MPa)	370	330	115	50
Tangent modulus(GPa)	23.5	22	19.8	17
Thermal conductivity(W/m°C)	120	134	146	159
Specific Heat(J/kg°C)	860	920	980	1050

The temperature rises at the contact interface due to frictional contact between the tool and workpieces. FSW generally occurs when the temperature at the weld line region reaches 70 to 90 percent of the melting temperature of the workpiece material [10].

A moving heat source was used to simulate the heat generated by friction. Meanwhile, a moving pressure of 1.5kN is applied synchronously to simulate the forging pressure of tool.

According to reference [11] and [12], the heat flux density of shoulder is expressed as,

$$q_s = \frac{\pi\omega\mu P(R_1^2 + R_1R_2 + R_2^2)}{45(R_1 + R_2)}, \quad (3)$$

and the heat flux density of stirring pin is,

$$q_p = \frac{\pi\omega\mu PR_2(1.5h+1)}{45}. \quad (4)$$

where,

$\omega$  : Rotating speed of tool,       $\mu$  : Friction coefficient,       $P$  : Forging pressure of tool,  
 $R_1$  : Radius of shoulder,       $R_2$  : Radius of stirring pin,       $h$  : Height of stirring pin.

The boundary conditions include thermal boundary conditions and mechanical boundary conditions. On the top and side surfaces of the workpiece, convection and radiation account for heat loss to the ambient [4], the value of the convection coefficient is set as 30 W/m<sup>2</sup>°C. Conduction losses also occur from the bottom surface of the workpiece to the backing plate, and a high heat-transfer coefficient of 300 W/m<sup>2</sup>°C is set. The workpiece is fixed by clamping plate [4], and the clamped portions are constrained in all directions. To simulate support at the bottom of the backing plate, all bottom nodes of the workpiece are constrained in the Z direction.

The simulated FSW process consists of three primary phases: dwell, traverse and cool. Three load

steps are applied corresponding with the three phases. Dwell phase means the heat source dwells at the initial position until the temperature reaches to the value required for the welding. Traverse phase means the rotating tool moves along the welding line, this is the most important phase during FSW. During the cool phase, the temperature of workpiece drops to initial value (25 °C) and then the fixture will be removed; accurate residual stress of FSW joint will be obtained after this phase.

The temperature distribution during the second load step is shown in Fig.9. The melting temperature of aluminum alloy 2524 is about 550°C, and the maximum temperature at the welding line is well below it.

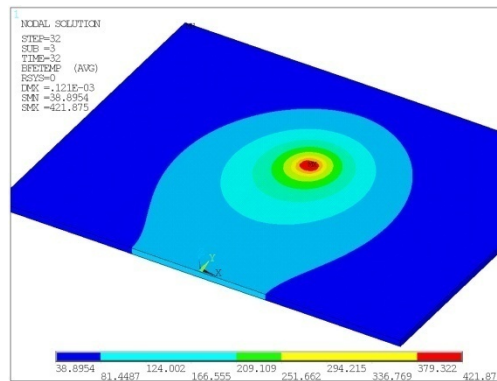


Figure 9. Temperature distribution during load step 2

The distribution of residual stress (X direction) after the third load step is shown in Fig.10. The residual stress distribution of middle site is different from that of the beginning and ending site. Because the FSW joint specimens are cut out from a big workpiece, the residual stress distribution of specimens can be considered as that of middle site.

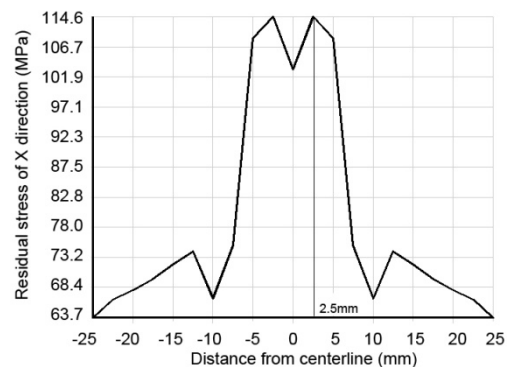
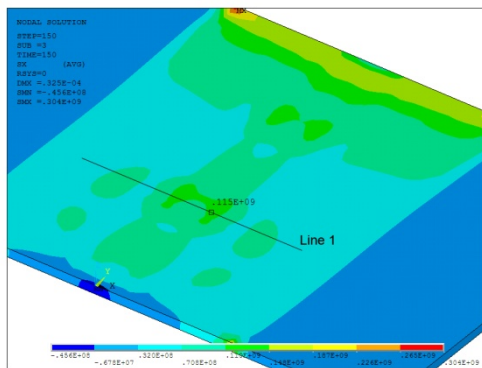


Figure 10. Distribution of residual stress (X direction) Figure 11. The residual stress distribution of line 1

Fig.11 shows the distribution of residual stress of line 1 (Fig.10). The maximum stress is 115MPa at the point of 2.5mm from the weld center, which shows a good agreement to the fracture position of FSW specimen.

### 3.2 FEA of lap joint

Three-dimensional lap joint specimen model is created as shown in Fig.12. The full scale joint is modeled considering the features of material nonlinearity, out-of-plane bending, pin-load and friction contact.

Both the pieces and rivets are meshed by 10 nodes tetrahedron solid element SOLID92. All the possible contact areas are modeled, and the rivets are modeled as ‘neat fit’ to holes and plates. The surface of model has the same displacement restriction as the specimen for the best boundary condition approximation.

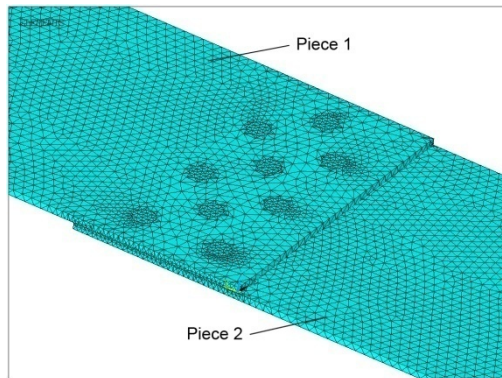


Figure 12. Finite element model of lap joint specimen

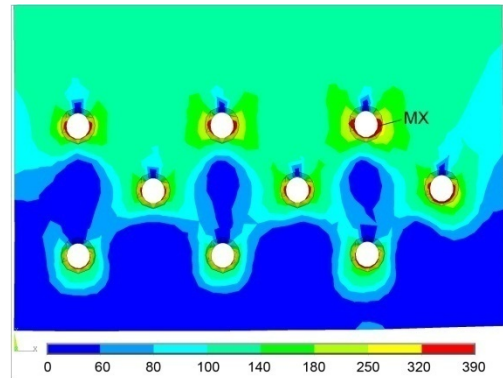


Figure 13. Von Mises stress of piece 1

Three-DOF constrain was applied on one side of the model, and pulling stress (120MPa) was evenly applied on the other side. Fig.13 shows the stress distribution of piece 1.

The maximum stress concentration of lap joint locates on the right hole’s edge of the first rivets row, it shows an excellent accordance with the crack initiation locations observed in tests. The maximum stress is 385MPa and the maximum strain is 0.0068 when the pulling stress is 120MPa; the maximum stress is 59.8MPa and the maximum strain is 0.00088 when the pulling stress is 7.2MPa.

## 4. Fatigue life estimate

In order to verify the validity of simulation method and establish links between FEA and test, fatigue lives of two different joints were estimated.

### 4.1 Fatigue life estimate of FSW joint

The fatigue life of FSW joint is estimated according to residual stress result and base metal S-N curve [9] on the bridge of *Goodman formula*.

We have known that the maximum residual stress of FSW joint is 115MPa. When the FSW joint under the constant amplitude load spectrum which maximum stress is 180MPa and stress ratio is 0.06 (accord to Fig.7, the fatigue life is 224566), the maximum local stress of joint is 295MPa

( $\sigma'_{\max} = 180 + 115$ ) and the stress ratio is 0.42 ( $R' = \frac{180 \times 0.06 + 115}{180 + 115}$ ).

Assume the decline of fatigue performance of FSW joint is only affected by residual stress. We can estimate the fatigue life of FSW joint by base metal S-N curve according to the maximum local stress of FSW joint.

*Goodman formula* is used to establish the relationship between the maximum local stress and the base metal S-N curve. *Goodman formula* is a constant life formula, which is expressed as,

$$S_a = S_{-1} \left[ 1 - \frac{S_m}{\sigma_b} \right]. \quad (5)$$

where,

$S_a$  : The stress amplitude of load spectrum,                       $S_m$  : The mean stress of load spectrum,

$S_{-1}$  : Stress amplitude when the stress ratio is -1,                       $\sigma_b$  : The ultimate strength of material.

Through calculation, the fatigue life of FSW joint is equal to that of base material specimen under the constant amplitude load spectrum which maximum stress is 247.6MPa and stress ratio is 0.06.

According to Fig.4 in reference [9], the fatigue life of base material specimen which considering the influence of residual stress is 252674 cycles, with an error of 12.5%. This result is basically identical with the experimental one, means that the residual stress is the main factor affecting the fatigue life of FSW joint.

#### 4.2 Fatigue life estimate of lap joint

The fatigue life of lap joint is estimated according to stress-strain results and *local stress-strain method*. Calculation formulas of *local stress-strain method* are shown as,

$$\varepsilon_a = (\varepsilon_{\max} - \varepsilon_{\min}) / 2, \quad (6)$$

$$\sigma_m = (\sigma_{\max} + \sigma_{\min}) / 2, \quad (7)$$

$$\varepsilon_a = \frac{\sigma_f' - \sigma_m}{E} (2N)^b + \varepsilon_f' (2N)^c. \quad (8)$$

where,

$\varepsilon_{\max}$ ,  $\varepsilon_{\min}$  : The maximum and minimum strain,                       $\sigma_f'$ ,  $\varepsilon_f'$ ,  $E$ ,  $b$ ,  $c$  : Material parameter,

$\sigma_{\max}$ ,  $\sigma_{\min}$  : The maximum and minimum stress,                       $N$  : Fatigue life.

According to the simulation results of FEA, the fatigue life of lap joint is 90400 cycles under the constant amplitude load spectrum which maximum stress is 120MPa and stress ratio is 0.06. The



estimate error is 8.2%, which satisfies engineering demands. The coincidence of estimate result and test result prove that the failure of lap joint is mainly caused by stress concentration of hole edge.

## 5. Conclusions

This paper has studied the fatigue properties of aerial aluminum alloy 2524-T3 FSW joint and lap joint by fatigue tests and FEA.

The S-N curves of different specimens have been obtained by fatigue tests to compare the fatigue strength of them. It has been shown that the fatigue strength of FSW joint is better than that of lap joint. At the fatigue life of  $1 \times 10^5$  cycles, the fatigue strength of FSW joints is about 61% higher than that of lap joint.

The three-dimensional elasticplastic FEA for two types of specimens have been developed to explore the fracture mechanism of two jointing techniques. The residual stress of FSW joint were obtained by a nonlinear direct coupled-field analysis, and the detailed stress distribution of lap joint which under pulling force were simulated. The maximum residual stress of FSW joint is 115MPa at the point of 2.5mm from the weld center, and the maximum stress concentration of lap joint locates on the right hole's edge of the first rivets row.

Finally, fatigue lives of specimens have been estimated, and both estimated results agree with that of experiment. Results show that the residual stress is the main factor affecting the fatigue life of FSW joint and the failure of lap joint is mainly caused by stress concentration of hole edge.

## References

- [1] W.M. Thomas, E.D. Nicholas, J.C. Need ham, M.G. Murch, P. Templesmith, C.J. Dawes, Friction Stir Welding, International Patent Application No. PCT/GB92102203 and Great Britain Patent Application No. 9125978.8, 1991
- [2] Alves de Sousa RJ, Yoon JW, Cardoso RPR, Fontes Valente RA, On the used of a reduced enhanced solid-shell finite element for sheet metal forming applications. *Int J Plasticity*, 23(2007) 490-515.
- [3] H.W. Zhang, Z. Zhang, J.T. Chen, The finite element simulation of the friction stir welding process. *Materials Science and Engineering A*, 403 (2005) 340-348.
- [4] Zhu X.K.,and Y.J.Chao, Numerical Simulation of Transient Temperature and Residual Stresses in Friction Stir Welding of 304L Stainless Steel. *Journal of Materials Processing Technology*, 146.2(2004)263-272.
- [5] Z. Feng, X.L. Wang, S.A. David, et al, Modelling of residual stresses and property distributions in friction stir welds of aluminium alloy 6061-T6. *Science and Technology of Welding and Joining*, 4(2007)348-356.
- [6] G.J. Bendzsak, C.B. Smith, An experimentally validated 3D model for friction stir welding, *Proceedings of the Second International Symposium on Friction Stir Welding*. Gothenburg, Sweden: TWI, 2000.
- [7] T. li, Q.Y. Shi, H.K. Li, Residual stresses simulation for friction stir welded joint. *Science and Technology of Welding and Joining*, 8(2007)634-640.
- [8] Zhou Caizhi, Yang Xinqi, Luan Guohong, Research Progress on the Fatigue Behavior of

- Friction Stir Welded Joints. *Rare Metal Materials And Engineering*, 7(2006) 1172-1176.
- [9] Zhang Teng, He Yuting, Wu Liming, Wang Xinbo, Fatigue Performance of Friction Stir Welded Butt Joints for 2524-T3 Aluminum Alloy. *Materials for Mechanical Engineering*, 5(2012) 47-49.
- [10] Prasanna P., B.S. Rao, G.K. Rao, Finite Element Modeling for Maximum Temperature in Friction Stir Welding and its Validation. *Journal of Advanced Manufacturing Technology*, 51(2010)925-933.
- [11] H.Schmidt, J.Hattel, J.Wert, An analytical model for the heat generation in friction stir welding Model. *Simul.Mater.Sci.Eng*, 12(2004)143-157.
- [12] Wang Jianhua, Yao Shun, Wei Liangwu, Thermal and thermo-mechanical modeling of friction stir welding. *Transactions Of The Chian Welding Institution*, 4(2002)61-64.
- [13] Chen Chuanrao, *Fatigue and Fracture* , Huazhong University of Sicence and Technology Press, Wu Han, 2001.